IEEE Access
Multidisciplinary | Rapid Review | Open Access Journal

Received June 25, 2019, accepted July 28, 2019, date of publication August 9, 2019, date of current version August 23, 2019.

Digital Object Identifier 10.1109/ACCESS.2019.2934385

Coordinated Dynamic Spectrum Sharing for 5G and Beyond Cellular Networks

JEONGHO JEON, RUSSELL D. FORD, (Member, IEEE), VISHNU V. RATNAM, (Member, IEEE), JOONYOUNG CHO, AND JIANZHONG ZHANG, (Fellow, IEEE)
Standards and Mobility Innovation Laboratory, Samsung Research America, Mountain View, CA 94043, USA
Corresponding author: Jeongho Jeon (jeongho.j@samsung.com)

ABSTRACT Current trends in spectrum regulation show that more and more unlicensed and shared spectrum bands are poised to be opened up for mobile communication. However, the question remains how to best utilize this spectrum and build efficient networks, and if the time has come for newer approaches to be considered for the next generation system. In this work, we propose a coordinated shared spectrum framework that can be considered for next generation cellular standardization. In designing the framework, we aim to improve upon the current unlicensed access schemes toward increasing spectral efficiency in highly-dense networks. To this end, we demonstrate that with the proposed framework both throughput and access delay can be significantly improved over the state-of-the-art LAA system. Also, by optimizing access delay and improving inter-operator resource fairness, the system is designed to be more amenable for operators to invest in deploying networks using shared spectrum. We further show that, by taking advantage of small timescale variations in traffic demand, large statistical multiplexing gains are possible through dynamic sharing instead of static, hard splitting of shared spectrum, as in the current CBRS system.

INDEX TERMS Coordinated spectrum access, dynamic spectrum access, shared spectrum.

I. INTRODUCTION

5G cellular network technology, known as New Radio (NR), is currently becoming a reality. The Third Generation Partnership Project (3GPP),[1] the organization responsible for 5G New Radio (NR) standardization, has completed the first phase of system design for NR in its Release 15 specifications (finalized in June 2018) and is currently conducting the second phase of standardization on additional enhancements in its Release 16 (to end in December 2019). With the NR standard now released, the first wave of 5G-enabled devices are being launched as operators worldwide start to deploy their 5G networks to bring subscribers fast and ubiquitous mobile connectivity.

Thus far, the NR standardization has been driven by new use cases, namely ultra-reliable low-latency communications and massive machine-type communications in addition to the conventional enhanced mobile broadband, and by new spectrum opportunities such as mmWave frequency bands. More recently, 3GPP has also been conducting standardization to support NR operation in unlicensed spectrum in Release 16, as an advancement of the LTE Licensed Assisted Access (LAA) [2]. As the fundamental wireless technology matures, it can be presumed that new use cases and new frequency opportunities will continue to drive the coming generations of cellular communications.

Presently in the United States, the Federal Communications Commission (FCC) is expanding the spectrum available for unlicensed and shared usage. For instance, the $3.55-3.7$ GHz Citizen's Broadband Radio Service (CBRS) band has been opened for shared access under a unique three-tiered access model, which consists of incumbents (federal government and fixed satellite service users), priority access licensees (PALs), and general authorized access (GAA) users, in descending order of priority [3]. GAA commercial service is expected to begin late this year and PAL auction and services are expected to begin from 2020. Additionally, in the US, the $5925-7125$ MHz (6 GHz) band is being considered for unlicensed use, whereas the $5925-6425$ MHz range is being considered in the EU. Regulations for the 6 GHz operation are expected to be finished in the 2019-2020 time frame [4]. The $37-37.6$ GHz band is also being considered for coordinated co-primary

The associate editor coordinating the review of this article and approving it for publication was Wen Chen.

[1] 3GPP has been the development hub of GSM (2G), UMTS (3G), LTE (4G) and NR (5G) standards [1].

shared access between federal and non-federal users [5]. In the case of the 60 GHz unlicensed band, the original 57−64 GHz range has been expanded to include 64−71 GHz. More recently, the FCC's Spectrum Horizon project is further pushing the outermost edge of usable spectrum into the Terahertz (THz) range [6]. A new category of experimental licenses for 95 GHz to 3 THz has been created and a total of 21.2 GHz of spectrum (116 − 123 GHz, 174.8 − 182 GHz, 185 − 190 GHz, and 244 − 246 GHz) has been made available for unlicensed use. A total of 102.2 GHz spectrum is being considered for licensed fixed point-to-point and mobile services, as well. Based on these trends, it is expected that more quantities of unlicensed and shared spectrum will be made available in the near future. Meanwhile, new advances are enabling wireless technology to push the upper reaches of the usable spectrum into higher frequency ranges, which until recent years were believed to be virtually unusable and impractical for mobile systems [7].

For existing unlicensed spectrum, an important issue faced by newly-introduced systems is that they must coexist with, and are subordinate to, already-operating incumbent systems. For instance, in the 5 GHz unlicensed band, new systems such as LTE LAA must conform to the same channel access mechanisms as the incumbent Wi-Fi technology, thus limiting their possible design choices. The carrier sense multiple access with collision avoidance (CSMA/CA) scheme used by Wi-Fi, although extremely successful in sparse or small local area networks, has been known to suffer from degraded performance in denser networks [8]. This has been the motivation the development of next generation Wi-Fi technology IEEE 802.11ax, also called High Efficiency WLAN during its early development.

Shared spectrum has been an active area of research for the past decade in the academic community. Only in recent years, however, has the industry started to come together to develop a commercial system standard. Following the opening of the CBRS band, the CBRS Alliance's work has been focused mainly around the operation and interfaces of the so-called Coexistence Manager entity, which is responsible for semi-statically allocating non-interfering channels to different GAA systems from a pool of GAA channels [9]. Unlike in fully dynamic access schemes like Wi-Fi and LAA, this semi-static, hard splitting of frequency resources does not allow fast resource reallocation between devices or operators and can lead to inefficiency and under-utilization of resources. Furthermore, the strict three-tier hierarchy presents an issue of accessibility for lower priority systems, which are barred from using the channel when higher-priority systems are operating.

This paper deals with the application of spectrum sharing technology to 5G and beyond cellular communication networks. Our interest is directed towards new unlicensed and/or shared spectrum, where the absence of existing incumbent systems presents the opportunity for new, greenfield channel access schemes to be developed. We argue that, in order to maximize spectrum utilization, dynamic sharing between localized sharing entities (devices and/or MNO networks) should be preferred over semi-static channel assignment by a centralized database. On the other hand, avoiding the inefficiencies of today's distributed access mechanisms, i.e., CSMA-CA, is one important design criterion to consider. Additionally, we explore more flexible approaches for prioritization of shared spectrum access, which will enable new business models and incentivize operators to adopt the technology for deploying their networks. Accordingly, in this paper, a Coordinated Spectrum Sharing (CSS) framework is proposed, which moves away from the use of listen-before-talk (LBT) and is based on dynamic coordination between base stations (BSs) that may belong to different mobile network operators (MNOs). The proposed framework allows soft prioritization between sharing entities, enabling a wide range of options from rigid hard prioritization to equal sharing. The outline of this paper is as follows. In the following section, we present an overview of the related standards and our research direction. In Section III, the proposed CSS framework is described in detail. In Section IV, the proposed CSS framework is evaluated in comparison with aforementioned existing technologies through simulation study. Finally, we summarize the key results and conclusions of this paper in Section V.

II. RELATED STANDARDIZATION AND OUR DIRECTION

A. CELLULAR UNLICENSED TECHNOLOGIES

Unlicensed LTE operation was introduced with the LAA system in the 3GPP Release 13 standard [10].[2] As the name LAA suggests, it cannot operate solely in the unlicensed spectrum but must be supplementary to a licensed carrier in the carrier aggregation (CA) mode. On the other hand, MulteFire has been developed for standalone unlicensed operation without the requirement for a licensed carrier [11].[3] Such a standalone system enables new business models and is attractive to non-conventional operators that do not possess licensed spectrum. Meanwhile, 3GPP is defining NR operation in unlicensed spectrum, namely NR-U, in Release 16 as part of NR phase 2 standardization [12]. Various operation scenarios are being considered, including carrier aggregation between licensed band NR and NR-U, dual connectivity between licensed LTE and NR-U, standalone NR-U, etc.

The aforementioned unlicensed cellular technologies were designed assuming the 5 GHz unlicensed band as the main target, although they are not fundamentally limited to operate in that band. IEEE 802.11 a/n/ac Wi-Fi technologies, operating in the 5 GHz band, use a channel access mechanism based on CSMA/CA with exponential random backoff.

[2]Release 13 LAA introduced downlink (DL)-only access, Release 14 enhanced LAA (eLAA) brought about uplink (UL) access and Release 15, with further enhanced LAA (FeLAA), enabled autonomous UL access to unlicensed spectrum [10].

[3]The MulteFire standard has not been developed independently from LAA; Common technical aspects are based on 3GPP's LTE LAA specifications and additional aspects of Multefire are only defined for unlicensed standalone operation.

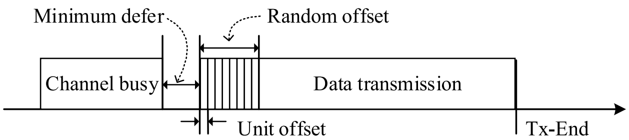

FIGURE 1. Listen-before-talk with random backoff.

An example channel access timing diagram is illustrated in Figure 1. Accordingly, the channel access mechanism for LAA/MulteFire/NR-U systems has been chosen to be analogous to that of Wi-Fi in the 5 GHz band due to concerns on fair coexistence with the incumbents. A key issue for Wi-Fi-like channel access is that it is difficult to predict upcoming access opportunities and a system may incur long delays in accessing the channel if it is in use by neighboring devices. Also, Wi-Fi-like systems exclude the possibility of explicit cooperation and coordination between devices. Nonetheless, despite these drawbacks, LAA was required to follow this scheme in order to coexist fairly with the incumbents.

B. CBRS SPECTRUM SHARING

The rulemaking around the CBRS band is nearing completion [3]. In a recent amendment, the unit of geographic area for PAL license was increased from census tract,[4] as previously proposed, to county. The license term was also increased to ten years from the original three years. These changes can be viewed as being in favor of MNOs using PAL, although they have, in effect, rendered the PAL system virtually not different from conventional licensed spectrum. Despite being more amenable to cellular network deployment by MNOs, with the current rigid three-tiered hierarchy of the CBRS band, the service continuity of PAL and GAA systems may not be guaranteed due to the uncertainty of spectrum accessibility. At the same time, the spectrum is assigned and managed by the central Spectrum Access System database, which can only adapt to varying utilization of the spectrum by reassigning channels over a relatively long timescale. Thus dynamic and agile sharing is difficult in the current framework.

C. CORRELATION OF TRAFFIC DEMAND AND OUR APPROACH

Prior to developing a spectrum sharing mechanism, the opportunities for sharing first need to be considered. The traffic demand, which in turn leads to the demand for spectrum, is mostly concentrated in urban areas. In other words, most MNOs are in need of more spectrum in urban areas and, conversely, most spectrum in suburban and rural areas is underutilized.[5] This claim is supported by the high correlation of LTE coverage maps between major US cellular operators, as shown in Figure 2. In addition, since humans are the main consumer of mobile data, traffic demand tends to follow the human diurnal cycle [14]. Consequently, most MNOs need more spectrum during peak hours and underutilize their spectrum during off-peak hours. Thus, given that traffic demand among MNOs is highly correlated both in time and location, there remains limited opportunity for spectrum sharing when and where the spectrum is the most needed. Although there is little sharing opportunity over a relatively longer time scale, e.g., an hour, when observed over microscopic timescales, MNOs exhibit quite non-uniform transmission patterns [15]. Moreover, with increasing demand for machine-type communications, the temporal traffic pattern may deviate from the human diurnal pattern in the near future, thus providing more opportunity for spectrum sharing.

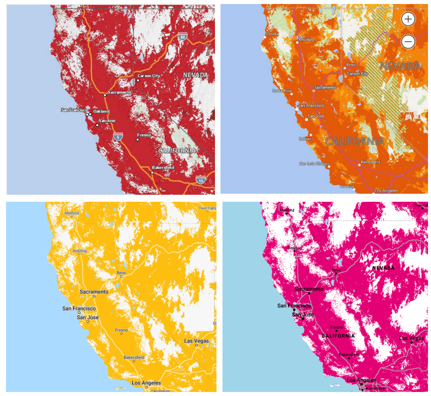

FIGURE 2. US west coast LTE coverage maps from major cellular MNOs.

Our interest lies in the sharing of spectrum between cellular MNOs in the most demanding scenarios. Our design exploits the spectrum sharing opportunities at microscopic timescales by applying an instantaneous, dynamic sharing framework.[6] Additionally, we propose a cooperative sharing mechanism that largely eliminates the need for CSMA/CA based channel sensing. As a result, we envision a system that can more effectively alleviate the surging demand for mobile data through offloading to shared spectrum and enable non-traditional operators to enter the market without the need for costly exclusive licenses.

III. COORDINATED SPECTRUM SHARING FRAMEWORK

A. MODEL AND ASSUMPTIONS

We consider a scenario where multiple BSs, possibly in close proximity, share a common spectrum. Moreover, the BSs may belong to different MNO networks. We introduce a new network entity called the Spectrum Sharing Manager (SSM). The SSM may be operated by some neutral party and may not belong to any one operator. In this paper, we propose both a

[4] Census Bureau data for 2007 indicate that there were 89,527 governmental jurisdictions in the United States [13].

[5] The coverage issue in suburban and rural areas results from the insufficient network infrastructure rather than spectrum shortage. Underutilized spectrum in suburban/rural areas can be compensated by sharing with applications such as smart farming.

[6] As an example, in the case of NR sub-6 GHz, depending on the 15/30/60 kHz OFDM subcarrier spacing, there are 1000/2000/4000 slots per second, which can be the number of spectrum sharing opportunities between MNOs per second [16].

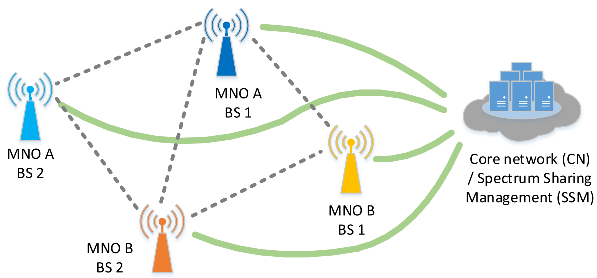

FIGURE 3. Example system model with spectrum sharing management entity.

distributed and centralized CSS framework and, depending on the approach, the scope of the SSM's role can be different. Figure 3 illustrates an example of the system model just described.

Ideally, BSs that strongly interfere with one another should use orthogonal resources, while BSs that do not cause much mutual interference can simultaneously access the same resource. In this paper, BSs are said to have an *interfering relationship* in the former case, whereas they are in a *non-interfering relationship* in the latter. One option to orthogonalize resources is simply to split the frequency range between interfering BSs, as done in the CBRS system. However, from the perspective of providing a multiplexing gain by allowing a temporarily unused resource of one BS to be utilized by another, we argue that time domain multiplexing will be superior to frequency division, which is the approach taken in the proposed CSS scheme. This claim will be further expounded and validated through simulation in Section IV.

In this work, we treat the resource reservation between BSs as being decoupled from the instantaneous scheduling decisions performed by each BS on how to utilize the reserved resource for, e.g., determining the transmission direction (DL or UL), which UEs to serve, etc. Certainly, the actual interference will depend on the transmission direction and the position of the receiver (a given UE in DL or the BS itself in UL). However, considering that scheduling decisions can change from one transmission time interval (TTI) to another and multiple UEs can be scheduled within one TTI in OFDMA systems, the interference conditions may be highly variable between TTIs. It would be quite challenging, from an operational complexity standpoint, to take the interference of individual BS-to-UE links (according to instantaneous scheduling decisions) into account when reserving the resource for different BS transmissions. Also, considering the amount of information exchanges (such as UE channel state information) that would be required, such an approach would be impractical. With this in mind, the proposed CSS framework instead aims to divide the resource in the time domain between adjacent BSs based on the interference relationships between the BSs themselves. Once a BS has reserved the resource, it is free to unilaterally decide how to utilize it. Then, if needed, the protection of a transmission at the receiver side can be enhanced with a receiver-based channel sensing mechanism similar to Request-to-Send/Clear-to-Send (RTS/CTS) in Wi-Fi. Lastly, time synchronization between BSs is assumed. Designing a solution for the over-the-air inter-BS synchronization has been a part of this research but omitted in this paper due to space constraints.

B. OVERALL FRAME STRUCTURE

In the proposed distributed CSS framework, the transmission is assumed to be temporally divided into frames. In the beginning of each frame, adjacent BSs exchange coordination signals over the air to (i) identify interference relationships and (ii) determine the intention of other BSs to access the spectrum. After these coordination signals are exchanged, each BS locally reserves a portion of the resource in the time domain and executes the actual data transmission. The overall frame structure, according to which this procedure takes place, is illustrated in Figure 4. The CSS frame structure consists of a Coordination Phase (CP) for signal exchanges and a Data Transmission Phase (DTP) for data transmission within the reserved resources. As shown in the figure, the CP is further divided into the Interaction Period (IP), Neighbor List Announcement Period (NLAP) and Reservation Announcement Period (RAP). In this paper, we explore both a distributed and a centralized design for the coordination among BSs. While the former design allows more prompt and flexible coordination between the BSs, the latter design requires no direct information exchange between the BSs, thus eliminating the CP overhead. Detailed operations during the CP will be explained through subsections III-C to III-E.

In the DTP, data transmission occurs according to the schedule reserved in the CP. Each DTP in Figure 4 has N DTP cycles, containing K slots each. Here a slot can be considered as equivalent to the basic TTI in LTE or NR. In this example frame structure, these K slots are reserved during the CP, and the slot pattern is repeated in each cycle. Doing so is advantageous from the perspective of reducing the signaling overhead for resource reservation compared to performing reservation for each cycle. That is, as the number of cycles N increases, the signaling overhead decreases. On the other hand, a smaller N allows for faster adaptation to the varying interference relationships, which may be caused by the variations in the channel and/or traffic demand over time.

C. DISTRIBUTED COORDINATION AND RESOURCE RESERVATION

In the IP, each BS is assigned a designated slot in which a Coordination Request (C-REQ) signal is sent, which may be followed by Coordination Response (C-REP) signal(s) from neighboring BS(s). The C-REQ can be a signal that simply encodes the transmitting BS's ID. If an OFDM waveform is assumed, the C-REQ can, for instance, be signaled by on/off modulation of a subcarrier tone, where the corresponding subcarrier index conveys the transmitting BS's ID. The C-REQ signal is transmitted with power P_{Tx}^{CP}, which is set

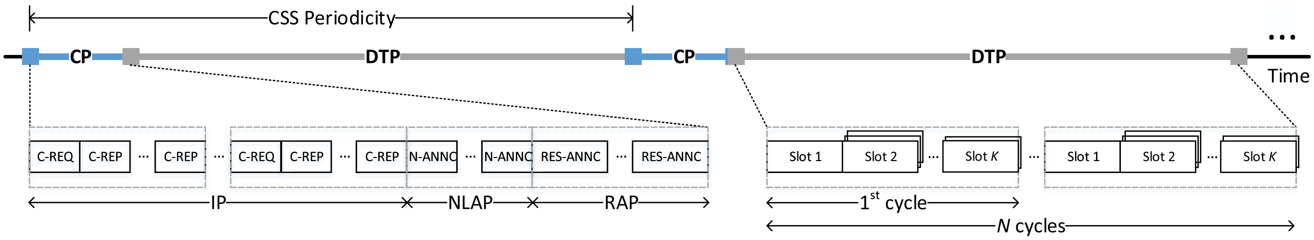

FIGURE 4. Distributed CSS frame structure.

Algorithm 1 Example CP Order Assignment Algorithm by SSM

1: Construct a interference graph $G = (V, E)$.
2: $i^* = \arg\max_{i \in V} |E_i|$.
3: $L \leftarrow |E_{i^*}| + 1$. ▷ Initial CP slot size.
4: **while** $\exists\, i^* \neq 0$ **do**
5:     **for** $\forall j \in V_{i^*}^1$ **do**
6:         **if** $\nexists$ a slot unassigned to V_j^2 **then**
7:             $L \leftarrow L + 1$
8:         Assign any slot unassigned to V_j^2 to j.
9:     $V = V \setminus V_{i^*}^1$.
10:     $i^* = \arg\max_{i \in V} |E_i|$.
11: **return** L and the assigned orders. ▷ Final CP slot size.

---

equal to the power intended to be used for the actual data transmission in the following DTP (denoted P_{Tx}^{DTP}). Upon receiving the C-REQ, neighboring BSs can estimate the expected interference level from the sender BS based on the received power of the signal. If a C-REQ signal is received at a neighboring BS with power exceeding a certain threshold, the neighboring BS responds to the sender by transmitting a C-REP signal.

Like with the C-REQ, with the OFDM signaling approach previously described, multiple neighboring BSs can embed their IDs in C-REP signals multiplexed in different subcarriers of the same OFDM symbol, which will reduce the signaling overhead compared to sending the signals sequentially. As the C-REP is only to indicate whether the C-REQ signal was received above a threshold, the C-REP need not depend on P_{Tx}^{DTP} and can be sent with higher power for more reliable reception.

The SSM can assign the order of transmitting the C-REQ/C-REP signals and/or the subcarrier positions, over multiple slots during the IP phase, to each BS by communicating with the operator core network (CN). In assigning the orders, the SSM may utilize the reported proximity or interference information between local BSs. Such information can be obtained by the SSM via periodic measurement reports send by each BS to the SSM with a list of neighboring BSs and their received signal strength. Note that such reporting to SSM by each BS may occur occasionally, while the distributed coordination between adjacent BSs is performed in every CSS periodicity to instantaneously recognize the varying interference level and the intention of transmission.

Algorithm 1 provides an example heuristic that can be considered to assign IP slots to the BSs, where each IP slot consists of a C-REQ followed by one or more C-REP signals. We assume that the SSM can construct the overall interference graph $G = (V, E)$ using the aforementioned periodic measurement reports, where the vertices V correspond to BSs and the edges E correspond to the interference relationship between a pair of vertices. Here, V_i^k denotes the set of vertices connected to node i in the k^{th}-hop or less (including vertex i) in G and E_i is the set of edges connected to vertex i. Next, the vertex i^* with the most edges is selected in step 2 and the number of slots L needed for the IP is computed based on the number of vertices adjacent to i^* including i^* itself in step 3. An IP transmission slot index can then be assigned to i^* and its neighbors. The heuristic proceeds by selecting the vertex with the next most edges among the vertices for which an IP slot index is yet unassigned and assigns an IP slot to this vertex and its neighbors as earlier described. In order to minimize the overall CP duration and thereby the overhead, already-assigned slots can be reassigned to BS j as long as the corresponding slots are neither used by its adjacent neighbors nor its two-hop neighbors, i.e., V_j^2, as described in step 6. The reason to avoid overlapping assignments between up to two-hop neighbors is to eliminate the possibility of C-REQ collision at any given BS such that no more than one neighbors use the same slot index. If a two-hop non-conflicting slot assignment is not possible with the current IP length L, L is increased by one in step 7. The above procedure is continued until all the BSs are assigned with an IP slot index. Slots in the NLAP and RAP phases can be assigned in the same fashion. It is noted that the above algorithm can be seen as an example solving the well-known scheduling problem in a conflict graph avoiding up to two-hop interference. Nonetheless, the algorithm is presented in this paper to exemplify how the IP slots can be assigned in the proposed CSS framework.

Let us now discuss on the threshold used to establish the interference relationships based on the received C-REQ signal strength. The criterion for a BS to acknowledge the interference relationship with another BS (and the decision to respond with a C-REP) is formulated as

$$P_{Rx}^{C-REQ} \geq TH\left(P_{Tx}^{DTP}\right), \tag{1}$$

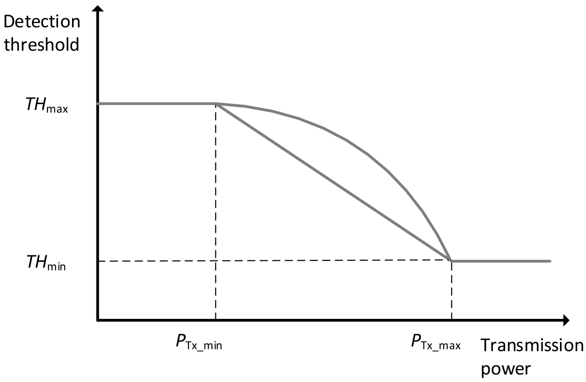

FIGURE 5. Example detection threshold function.

where P_{Rx}^{C-REQ} is the received C-REQ signal power at a BS and P_{Tx}^{DTP} is the intended transmission power during the DTP by the BS receiving the C-REQ. As exemplified in Figure 5, the threshold is a non-increasing function of P_{Tx}^{DTP} within a specified maximum and minimum value, denoted by $TH_{\max}$ and $TH_{\min}$, respectively.[7] The decision to respond with C-REP is thus not only based on the received C-REQ signal power but also the intended DTP transmission power of the responding BS. This reflects the requirement that, if a BS wishes to use a relatively high power for its data transmission, it should acknowledge its interference relationship with other BSs transmitting C-REQ, even though the received C-REQ power may be relatively low, as the high transmission power used by the BS can interfere with BSs from which the C-REQ is received. As a result, a BS intending to use higher transmission power would need to split the resources orthogonally with a larger set of BSs over a wider area. Conversely, if a BS indicates to use lower transmission power, it will acknowledge fewer interference relationships and will share the resource with a smaller set of neighbors at the cost of a smaller coverage area. The C-REQ/C-REP signal exchanges also serve as a method to indicate the intention of operation for the given CSS period. If a BS has no data to transmit/receive, it can inform neighboring BSs simply by not participating in the C-REQ/C-REP signal exchanges and, consequently, fewer BSs will split the resource.

Importantly, interference relationships must be mutually respected between a pair of BSs. If only one BS recognizes a neighbor as an interferer while the neighbor does not reciprocate, said BS needs not respect the neighbor in the subsequent resource reservation procedure. The confirmation of the mutual interference relationship is made in the NLAP phase by broadcasting the list of neighbors that the BS has sent the C-REP signal during the IP. The neighbor list announcement (NLA) can be a signal that encodes all the BSs' IDs on the neighbor list, again possibly with on/off signaling of subcarrier tones as previously discussed, where the correspondence between subcarrier indexes and BS IDs is indicated by SSM. Each BS would then compare its neighbor list with the lists received from its neighbors and, if an interference relationship is not respected by a neighbor, the corresponding BS is also free to neglect the relationship.

[7] A similar energy detection threshold function is defined in the EU for operations in the 5 GHz unlicensed band and adopted for LTE LAA, accordingly [17].

Algorithm 2 Example Distributed Resource Reservation Ratio Determination Algorithm by BS i

1: Construct a local interference graph $G_i = \left(V_i, \bar{E}_i\right)$.
2: Partition G_i into the set of fully-connected complete subgraphs $G_i^k = \left(V_i^k, E_i^k\right), k \in \{1, \ldots, K\}$.
3: $N_i = \max_k |V_i^k|$
4: $R_i = \alpha_i / N_i$. ▷ $\alpha_i :=$ priority factor of BS i.
5: **return** R_i ▷ Resulting reservation ratio of BS i.

Once the mutually-interfering neighboring BSs are identified, the fraction of DTP resources to be reserved by each BS, called the *reservation ratio*, can be computed. Although many approaches are possible and can be enforced by the SSM to BSs to follow in computing the reservation ratio (to maintain different notions of fairness, etc.), we present an example procedure in Algorithm 2, according to which each BS calculates the reservation ratio that is inversely proportional to its number of interference relationships. The proposed algorithm also enables *soft prioritization* between BSs of different MNOs when reserving the common shared spectrum. This enables MNOs to, for example, pay the spectrum regulation authority for preferential access to some fraction of the resource. Note that soft prioritization is distinguished from hard prioritization of CBRS in the sense that lower priority systems are not totally deprived of access to the channel and can still reserve some portion, depending on their priority level. Additionally, in the CSS framework, any system (regardless of its priority) can opportunistically access a resource reserved by another system if (i) it is not actually utilized or (ii) it can ensure that its interference to the reserved system is below a certain threshold. We thus introduce the concept of secondary opportunistic access in the following subsection.

By applying Algorithm 2, the resource reservation ratio can be determined in a distributed fashion by BSs independently. Through the NLAP, each BS will be aware of interference relationships between itself and its adjacent neighbors, as well as relationships between each of the neighbors by reading the broadcast neighbor lists. Thus, BS i can derive the local interference graph $G_i = \left(V_i, \bar{E}_i\right)$ centered at itself, where V_i denotes the set of vertices connected to node i including node i itself and the set $\bar{E}_i$ includes edges not only connected to node i but also between the one-hop neighbors of node i. Subsequently, BS i finds the largest *complete* subgraph[8] G_i^k from G_i. The largest complete subgraph of G_i

[8] Here, a complete subgraph, also referred to as a clique, is a subset of vertices that are fully interconnected between themselves.

relates to the most congested cluster of BSs and, therefore, the one for which the resource needs to be split the most among the neighbors of BS i. It is noted that by the definition of G_i, any complete subgraph will include BS i itself. Accordingly, the inverse of the total number of vertices in the largest complete subgraph equals the ratio that the corresponding BS can reserve the resource, if equal priority among BSs is assumed. The other neighboring BSs of i which are not in the largest complete subgraph can then spatially reuse the resources that are not reserved by BS i.

As explained earlier, the priorities between different MNOs may be different and, in such a case, different priority factors α_i in reserving the resource can be assigned by the SSM. The final reservation ratio is thus obtained by multiplying the priority factor α_i by the previously obtained reservation ratio. Each BS then reserves any unclaimed resource according to this ratio and announces it in its designated RAP slot.

Algorithm 2 is performed independently by each BS and the reservation is made sequentially according to the announcement order in RAP in Figure 4. In choosing the resource to reserve, a BS can spatially reuse the resource that is not reserved by its mutually-interfering neighbors, while the BS should avoid the resource that has been already reserved by any of the its mutually-interfering neighbors in earlier RAP slots. On the other hand, a BS, especially those whose announcement slot is later in RAP, may encounter that the remaining resources available for reservation may be less than the calculated reservation ratio. Such situation can be informed to SSM such that SSM can adjust the priority factors or shuffle the reservation announcement orders to resolve the shortage.

1) EXAMPLE

Consider the BS A in Figure 6. For the given connectivity graph in Figure 6a, subgraphs $\{A, B, C\}$ and $\{A, D, E\}$ are the two equally largest complete subgraphs of BS A and, thus, the reservation ratio turns out to be 1/3. This implies that 2/3 of the resource that is not reserved by A can be spatially reused by the neighbors of A, i.e., the sets $\{B, C\}$, $\{D, E\}$, and F, as they are non-interfering between them. When BSs are sequentially reserving the resources during RAP, it needs to avoid a resource that has been already reserved by its one-hop neighbors. Figure 6b shows the resulting DTP reservation after all BSs perform Algorithm 2 in a distributed manner, assuming an equal priority factor of $\alpha_i = 1$. In this example, it was assumed that the reservation announcement is made according to the alphabetic order, i.e., from A to I.

We note that there may be some corner cases, such as ring topologies with an odd number of nodes. Although this arrangement of interference relationships is unlikely to happen in wireless networks, all the nodes in this example would derive the reservation ratio of 1/2 and the last node in the reservation order will be left having no resource to reserve. This is another purpose of introducing the priority factor α_i. Upon detecting such situation through receiving feedback reports from BSs, the SSM can adjust α_i of neighboring nodes such that some fraction of resource is made available for all BSs.

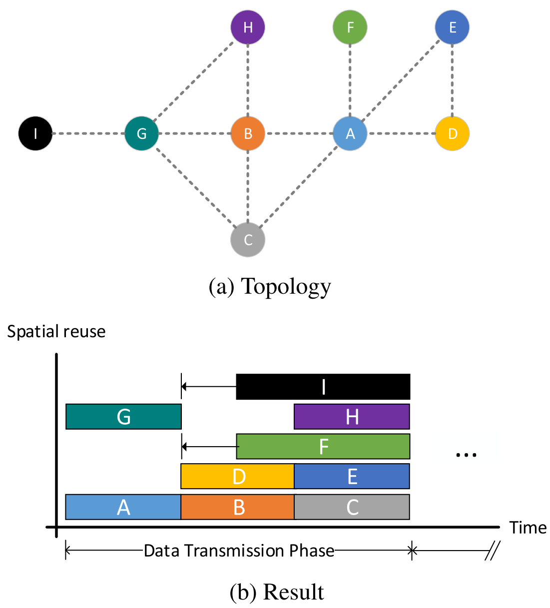

FIGURE 6. Example topology and resource reservation.

D. OPPORTUNISTIC SECONDARY ACCESS

In the proposed approach, in addition to the coordinated transmissions based on reservation, opportunistic channel access with LBT is allowed. Opportunistic transmission may be possible in the following cases: (1) A particular slot is not reserved by a neighbor in a mutual interference relationship, (2) a slot is reserved by at least one neighbor but is not actually used for transmission or (3) a slot is reserved by at least one neighbor and is used for transmission but a secondary BS can sufficiently limit its interference to the ongoing transmission through power control. Channel sensing is essential in all of the above cases. Whether to allow opportunistic secondary access can be determined if the following condition is satisfied:

$$P_{Rx}^{\max} \leq TH\left(P_{Tx}^{oppo}\right) - \delta, \tag{2}$$

where $P_{Rx}^{\max}$ is the maximum received power among the detected signals and P_{Tx}^{oppo} is the transmit power intended by a BS for opportunistic transmissions, which may be different from P_{Tx}^{DTP} of the BS intended to be used for its own reserved data transmission slots. The threshold function $TH(\cdot)$ is the same as in equation (1). Additionally, the margin δ may be assigned by the SSM to protect the *primary* BS having reserved the slot. If no transmission is performed as in the first two cases, the criterion in equation (2) will be met regardless of the value of δ. However, if there is a transmission by the primary BS, a larger δ implies that the secondary transmitter needs to further reduce its power to satisfy the condition. Accordingly, as δ increases, primary transmissions are more rigorously protected while overly restricting the secondary transmissions. Thus, there is a trade-off. The margin can furthermore be differentiated depending on whether the primary and potential secondary BSs belong to the same or different MNO and denoted as $\delta_{intra-op}$ and $\delta_{inter-op}$, respectively. By doing so, the allowance of opportunistic access can be restricted within the same MNO BSs.

As the secondary opportunistic transmissions are not coordinated in advance like reserved DTP transmissions, LBT needs to be performed as illustrated in Figure 1 before initiating a secondary transmission due to the possibility of collision. However, we propose several optimizations over conventional LBT schemes tailored to CSS framework. First, a defer duration at the beginning of the DTP slot ensures priority to the primary BS so that it can perform its transmission without channel sensing. If no transmission is detected above the threshold in equation (2), a potential secondary BS may continue channel sensing with a certain offset for collision avoidance between secondary transmissions. The offset can be randomly chosen within a certain range, e.g., within the first OFDM symbol,[9] or it can be deliberately chosen and preassigned by the SSM, possibly taking into account interference relationships and priorities of the secondary BSs. It is noted that the duration of secondary transmissions can be less than a full slot duration due to the initial symbol(s) set aside for channel sensing. In this case, mini-slots similar to NR can be utilized. In the case of LTE LAA, shortening the transmission via symbol puncturing or rate matching was considered.

The offset can be fixed, or it can be *drifted*, as in Wi-Fi or LAA, meaning that the sensing countdown is frozen when the channel is sensed busy and resumed when the channel is sensed idle again. Another aspect to note is that the channel sensing and opportunistic transmission must be confined within a given slot, as the primary transmission may resume or the BS having reserved the slots may change over consecutive slots. Thus, any secondary BS must terminate its transmission at the slot boundary and should perform sensing again to reconfirm the availability of the following slot.

E. CENTRALIZED CSS FRAMEWORK

The centralized CSS (C-CSS) framework is described in this subsection, focusing mainly on the differences with the distributed CSS (D-CSS) and avoiding duplicated description as much as possible. In the C-CSS framework, the resource reservation and allocation to individual BSs is performed by the SSM in a centralized manner, as opposed to in a decentralized fashion by CP signal exchanges. Accordingly, in Figure 4, the overall frame structure consists only of the DTP, while eliminating the CP. In order for the SSM to allocate the resource, it requires the knowledge of the global (network-wide) interference graph. Toward this end, coexistence measurement reports (CMRs) are employed by which each BS signals information to the SSM, such as the list of neighboring BSs and their received signal strength.

Based on CMRs from BSs, the SSM performs global resource allocation considering the interference relationship between adjacent BSs while maximizing the spatial resource reuse between non-interfering BSs, similar to Algorithm 2. After that, the allocation is informed to BSs along with the maximum allowed transmission power, which are enforced to obey. The CMR can be sent periodically and/or aperiodically triggered by certain predefined events. Further details on the content of CMR messages is given in the following subsection. As noted, with the elimination of CP overhead, the C-CSS resource utilization efficiency can be higher than D-CSS. However, as it is difficult to frequently reconfigure the resource allocation by SSM, which involves higher layer signaling from/to the core network, the C-CSS approach comes with the limitation of not being able to as flexibly adapt to varying interference conditions, varying transmit power levels and/or varying traffic demand compared to D-CSS. The opportunistic channel access previously described applies likewise to C-CSS as well as D-CSS.

F. NETWORK MANAGEMENT FUNCTION

In the following, some essential network management functions are introduced. Some aspects are commonly applicable to both distributed and centralized approaches, while some others may be applicable to only one or the other. The CMR from individual BSs to the SSM may include the following information:

- The list of neighboring BSs and their signal strength. In the D-CSS case, this information is used to assign the signal exchange order in the CP, while in the case of C-CSS, it may be directly utilized to allocate resources to BSs in DTP. In the case of C-CSS, the SSM can further infer, to some degree, the violation of the transmission power level from the maximum allowance.
- The reservation success ratio by which each BS can report the difference between the calculated reservation ratio and the actually reserved ratio, as explained earlier in Section III-C, for the D-CSS case.
- The channel occupancy and background interference level. This information can be utilized by the SSM to identify how heavily the channel is being used and to reallocate the channels, if necessary. (Similar information report was introduced for LTE LAA as a part of Release 13 Radio Resource Management enhancement.)

Based on the CMRs from BSs, the SSM makes decisions regarding network operation. The SSM can then configure the following parameters to the BSs:

- The CP structure including the transmission order, mapping between BS ID and subcarrier index, and the

[9] In NR with the 15 kHz subcarrier spacing, like LTE, one symbol duration is approximately 70 μs including the cyclic prefix. If we assume a 25 μs defer duration and 9 μs sensing slot duration similar to LTE LAA, there could be 5 sensing offsets created within one OFDM symbol including the initial defer duration. To have higher contention resolution, additional OFDM symbol(s) can be used to create more offsets.

TABLE 1. Simulation model parameters.

Parameter	Value
Radio Access Technologies	CBRS (w/ LTE), IEEE 802.11n/ac Wi-Fi, LAA, CSS (w/ LTE)
Topology	Clustered small cell deployment with 2 MNOs coexisting. BSs/UEs dropped uniformly randomly in the cluster of 50/70 m radius.
# of nodes (per MNO)	$N_{BS} \in \{5, 10, 10, 20, 25\}$ Average 2 UEs/BS
Inter-cell Distance	10 m
Cell assoc. method	Best Reference Signal Received Power (RSRP)
Carrier freq.	5 GHz
Bandwidth	20 MHz for CSS/LAA/Wi-Fi (shared channel) 10 MHz for CBRS (1 channel/MNO)
BS EIRP	23 dBm (18 dBm TX power + 5 dBi gain)
PD/ED Threshold	CBRS: N/A Wi-Fi: -82 dBm for PD/-62 dBm for ED LAA: -72 dBm for ED CSS: -52 dBm for ED
Channel model	Urban Micro (UMi)
Traffic (Downlink)	FB: Full Buffer NFB High load: FTP, 100 KB files, $\lambda = 4$ files/s NFB Low load: FTP, 100 KB files, $\lambda = 2$ files/s
MAC scheduling policy	Rate proportional-fair (LTE) Round robin (Wi-Fi)
Simulation duration	10 seconds
# drops (per test)	10

number of slots in the IP, NLAP, and RAP, for the D-CSS case.

- The DTP structure including the number of cycles N in the DTP and the number of slots K in each cycle.
- The allocated transmission schedule and the maximum allowed transmission power for data transmission for the C-CSS case.
- Priority factor α_i for resource reservation for the D-CSS case.
- Channel sensing related parameters including detection threshold function, the protection margin for the opportunistic secondary access, which can be separately configured for intra/inter-MNO cases as explained in Section III-D, and random sensing offset, etc.

IV. SIMULATION STUDY

In this section, we demonstrate the performance gains of CSS through system-level simulation, which is fully compliant with 3GPP performance evaluation methodology [18]. We compare the proposed centralized and decentralized CSS access schemes (with LTE as the underlying radio access technology) alongside LAA and Wi-Fi to quantify the benefits in terms of throughput and efficiency. Additionally, we simulate LTE over CBRS-GAA with fixed channel allocations. With this scenario, we intend to show the potential statistical multiplexing gains of CSS over CBRS thanks to exploiting small timescale traffic variations.

A. SIMULATION SETUP

We simulate deployments of small cell clusters following the configuration in Table 1. BSs for two MNOs are placed randomly in the same cluster with a 10 m minimum inter-BS distance. The number of BSs, denoted N_{BS}, is varied from 5 to 25 (in increments of 5) for each operator. The number of UE is $N_{UE} = 2N_{BS}$. The 3GPP Urban Micro (UMi) channel model is employed. Only downlink transmissions are simulated with both full-buffer (FB) and non-full buffer (NFB) traffic, where the 3GPP FTP traffic model is used in the latter case. For the CSS, LAA and Wi-Fi, we consider a scenario where the two MNOs share a single channel of 20 MHz bandwidth. For the CBRS-GAA scenario, each MNO is assigned their own 10 MHz channel for exclusive operation. This setup is intended to fairly demonstrate the trade-offs between fixed spectrum allocation in CBRS and fully-opportunistic, LBT-based access of LAA/Wi-Fi, and how the proposed CSS schemes incorporate elements of both to improve efficiency and performance.

In the simulation results discussed below, we compare each system in terms of the downlink user-perceived throughput (UPT) experienced by each UE. The UPT is defined as the total number of bits successfully received by a UE normalized by the amount of time that the DL buffer for the UE was non-empty during the simulation run. We are also interested in evaluating the average *access delay* experienced by each BS, which we define as the time taken to actually start a transmission from the instant that a BS has an intention to transmit. The access delay is an indicator of the latency from contention for channel access. Importantly, for shared spectrum systems, it is desirable for the access delay to be well-controlled and not be excessive or unpredictable due to the resource being in use by systems of other operators. Additionally, we are concerned with the *resource fairness* involved in accessing the channel, which may be defined in terms of Jain's fairness index as $J = \frac{1}{|\mathcal{K}|}(\sum_{k\in\mathcal{K}} t_k)^2/\sum_{k\in\mathcal{K}} t_k^2$, where t_k represents the fraction of time that cell k accesses the channel out of the total simulation run time. The fairness index takes values between 0 and 1 (the most fair) [19]. Note that this is time-domain resource fairness amongst BSs, not the rate fairness amongst UEs. The fairness index will be given for the FB case only as it is influenced by varying buffer occupancy in the case of NFB and therefore may not accurately convey the resource fairness.

On the other hand, the key difference between our modeling of the distributed and centralized CSS approaches in the simulation is that, with D-CSS, the DTP slot reservation pattern is refreshed every CSS cycle, whereas with C-CSS the slot allocation pattern is assigned to each BS only once at the beginning of the simulation based on the long-term statistics, after which the slot pattern is not updated.

B. SIMULATION RESULTS

1) SELECTION OF CSS ED THRESHOLD

As discussed in Section III, the choice of signal detection threshold function is central to the operation of both distributed and centralized CSS approaches. In Figure 7, we demonstrate the performance of the proposed CSS scheme under full buffer traffic over the signal detection thresholds

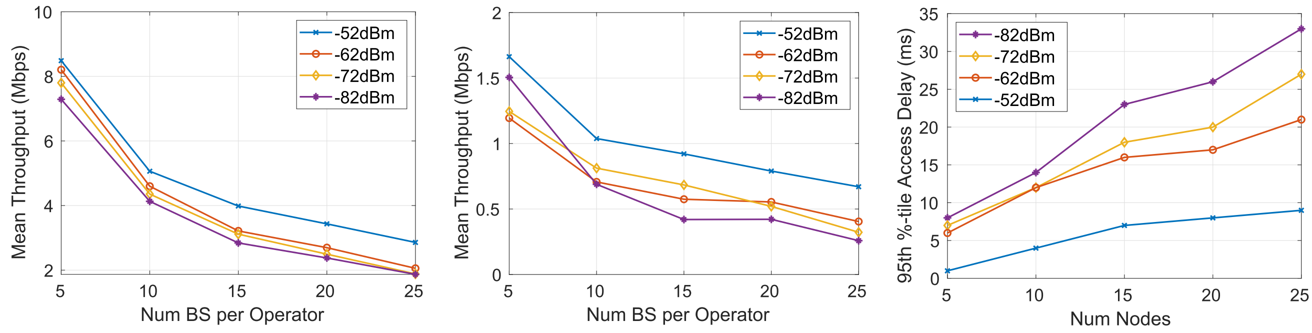

(a) Mean UPT (b) 5th-Percentile UPT (c) 95th-Percentile Access Delay

FIGURE 7. CSS performance for various ED thresholds.

between −82 dBm and −52 dBm, in increments of 10 dBm, in order to empirically determine the optimal operating threshold.

From the figures, the lowest, the most sensitive threshold of −82 dBm has the worst overall performance among the set of thresholds. Although this threshold reduces interference the most, it results in the most conservative sharing of the resource as the resource being divided excessively while limiting the spatial reuse. Thus, transmission opportunities for each BS are, in general, reduced and throughput and access delay are degraded in turn. We find that both mean and 5^{th}-percentile UPT performance continue to improve with less sensitive ED thresholds as a result of increasing the transmission opportunities. We note that, although the inter-cell interference does naturally increase with higher thresholds, the link adaptation capability of the LTE eNodeB scheduler is able to compensate so that packet error rate performance is not severely degraded and capacity is not significantly reduced. This trend continues until −52 dBm, beyond which the effect of reduced SINR becomes dominant over the improvement from increased transmission opportunities and the UPT performance, particularly at the cell edge, is sharply declined. Accordingly, −52 dBm is chosen as the best fixed threshold for the experiments in the following sections.

2) CSS VS. LAA/Wi-Fi

We first compare CSS to LAA and examine the scenario when the network becomes highly dense with 25 BSs per each of two MNOs. One observes around a 40% increase in mean UPT for CSS over LAA with FB traffic (Table 3), a 113% increase in the high load NFB traffic case (Figure 8a), and a 143% increase in the low load NFB traffic case (Figure 9a). This boost in throughput is attributed to the improved efficiency from avoiding excessive contention and collisions. One finds similar throughput gains (again in the 25 BS case) for the C-CSS scheme, although the mean UPT is marginally less than D-CSS. Even greater improvement is shown when compared to Wi-Fi.

While the gains in mean throughput are clear, the gains in cell edge (worst 5^{th}-percentile) UE UPT are even more

TABLE 2. Performance comparison with full buffer for 5 BSs/MNO.

Metrics	CBRS	Wi-Fi	LAA	CSS
Mean UPT (Mbps)	5.75	4.69	7.19	**8.49**
5^{th} %-tile UPT (Mbps)	1.47	0.17	0.05	**1.66**
95^{th} %-tile wait time (ms)	0	34	12	**1**
Resource fairness index	1.00	0.47	0.52	**0.88**

TABLE 3. Performance comparison with full buffer for 25 BSs/MNO.

Metrics	CBRS	Wi-Fi	LAA	CSS
Mean UPT (Mbps)	2.03	0.96	2.06	**2.86**
5^{th} %-tile UPT (Mbps)	0.62	0.11	0.13	**0.67**
95^{th} %-tile wait time (ms)	0	148	96	**9**
Resource fairness index	1.00	0.39	0.47	**0.81**

appreciable. Most notably, in Table 3, Figure 8b and Figure 9b, we see that CSS offers a 415% increase in cell edge UPT for FB traffic, a 60% increase for high-load NFB traffic and a 403% increase for low load NFB traffic compared to LAA. This result clearly demonstrates that edge UEs near the cell boundary are at a disadvantage with LBT-based technologies due to hidden node problem.[10] By managing interference between nodes more deliberately and avoiding collisions entirely, CSS can reduce interference seen by edge users.

CSS also exhibits improved performance even when the network is relatively less dense with 5 BSs per MNOs. In Table 2, we find over a 30 times increase in cell edge UPT over LAA and a 9 times increase compared to Wi-Fi for the 5 BS per operator scenario. On the other hand, the 95^{th}-percentile access delay decreases from 12 ms for LAA to less than 1 ms for D-CSS and FB traffic, and is only slightly higher for the C-CSS approach. While the access delay increases rapidly with the network density for both LAA and Wi-Fi, the change in delay is subtle, by comparison, for both CSS schemes and never exceeds 20 ms for both FB and NFB traffic. This is over a 90% decrease in access delay from LAA in the 25 BS case. Under FB traffic, CSS

[10]Receiver based channel sensing, e.g., RTS-CTS, is not assumed for LAA/Wi-Fi in the evaluation.

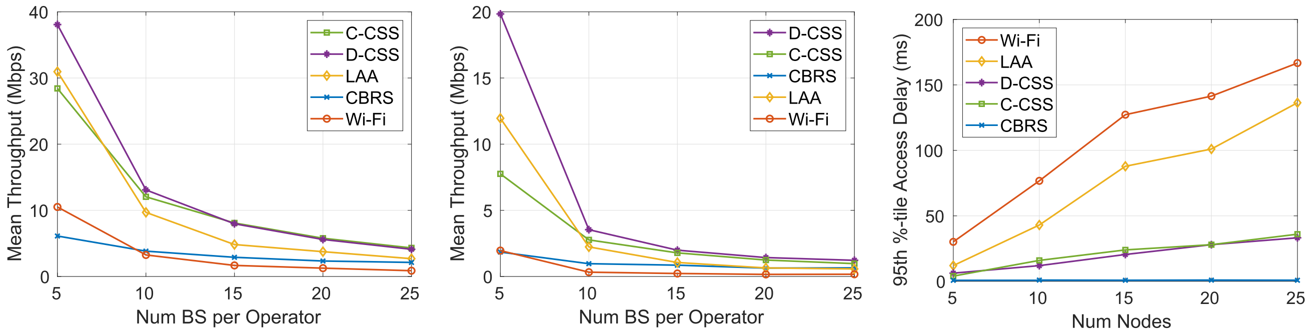

(a) Mean UPT (high load) (b) 5th-%tile UPT (high load) (c) 95th-%tile Access Delay (high load)

FIGURE 8. Performance comparison for high load NFB scenario with $\lambda = 4$.

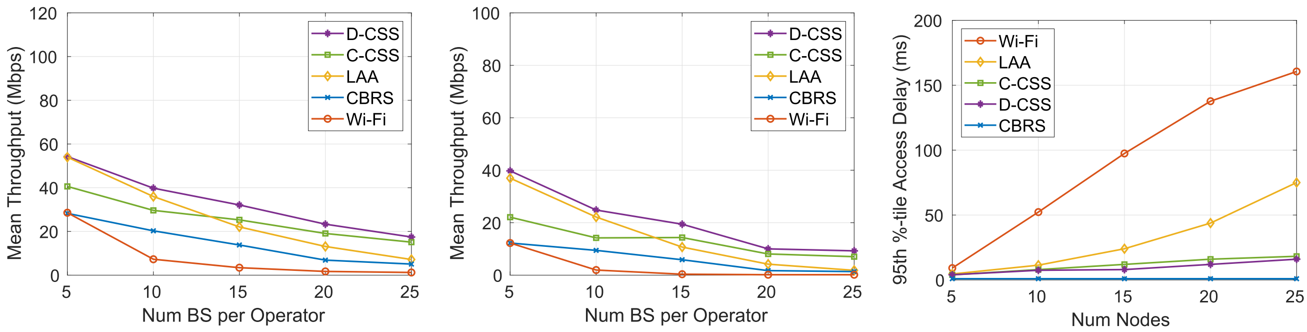

(a) Mean UPT (low load) (b) 5th-%tile UPT (low load) (c) 95th-%tile Access Delay (low load)

FIGURE 9. Performance comparison for low load NFB scenario with $\lambda = 2$.

eliminates the need to continually contend for the channel and reserves some portion of the resource for each BS at regular intervals. Less appreciable gains are seen for the low-density, low load case in Figure 9b, which is unsurprising since the number of active nodes at any time, and thereby the likelihood of contention, will be low.

The access delay also affects the short-term fairness of the system. Multiple access in both Wi-Fi and LAA is, in principle, designed to be perfectly fair asymptotically, in that no deliberate prioritization is given to any BS contending for access. However, in the short term, nodes that currently have access to the channel tend to hold on to the resource and prevent interfering nodes from initiating access, thus causing starvation. CSS, on the other hand, ensures that every node requesting access to the channel will be granted some fraction of slots in every DTP cycle. This effect is highlighted by the improved fairness index in Table 3.

3) CSS VS. CBRS

CSS provides large improvements in mean UPT over CBRS, with a 40% gain for FB traffic, 103% gain for high load NFB traffic and 243% gain for low load NFB traffic in the 25 BS case, as shown in Table 3, Figures 8a, and Figure 9a, respectively. Higher gains for NFB traffic are expected since, when the network is not heavily loaded, hard splitting of the bandwidth between MNOs can lead to a situation where some operators' bandwidth is underutilized and could be used opportunistically by another operator. In the FB scenarios, we find there is less of a gap between CBRS and CSS performance since each of the MNOs' channels are fully-loaded and there is no chance for a multiplexing gain by sharing the total resource.

Further impacting the performance of CBRS when networks densify is the high interference seen at the cell edge. It is well known that cell edge users inherently suffer under full frequency reuse, which has been the motivation for Inter-Cell Interference Coordination (ICIC) in LTE Release 8. The resource reservation approach in CSS avoids neighboring BSs reusing the same resource and, thus, offering a 576% gain at cell edge UPT versus CBRS in the low load FTP traffic case with 25 BSs (Figure 9b).

We note that the access delay and resource fairness of CBRS are intrinsically superior, since each operator has its own dedicated channel and the BSs can transmit in any subframe without delay under the assumption of frequency reuse factor 1. For this reason, the access delay is given as 0 and fairness index as 1 in Tables 2 /3.

Finally, for the case of D-CSS, it is admitted that the CP overhead would be challenging to quantify exactly as it depends on many implementation details and, thus, the results in this section do not yet account for this overhead. However, as discussed in Section III, the CP signal exchanges can be done in a compact format using tone-based signaling, so it is expected that the observations made in this section remain valid.

V. CONCLUDING REMARKS

With the culmination of 3GPP NR standardization and the launch of the first NR devices and networks, the 5G era is quickly approaching. As 5G was driven by the advent of new use cases and the availability of new spectrum bands, so will the next generation of wireless technology. Current trends in spectrum regulation show that more and more unlicensed and shared spectrum bands will be opened up. Thus, the time has come to answer how to efficiently utilize these new spectrum over today's CSMA-CA-based Wi-Fi and LAA systems, whose performance is known to degrade severely when networks become highly dense. To this end, we proposed a coordinated shared spectrum framework achieving increased spectral efficiency and reduced over-the-air latency and congestion. Also, by inherently taking access delay and fairness between operators into account, the system is designed to be more amenable for MNOs to invest in deploying networks using shared spectrum. In addition, it has been demonstrated that the proposed scheme can deliver large statistical multiplexing gain through dynamic sharing compared to CBRS system, which is based on static splitting of resources.

REFERENCES

[1] *The 3rd Generation Partnership Project*. [Online]. Available: http://www.3gpp.org/
[2] H.-J. Kwon, J. Jeon, A. Bhorkar, Q. Ye, H. Harada, Y. Jiang, L. Liu, S. Nagata, B. L. Ng, T. Novlan, J. Oh, and W. Yi, "Licensed-assisted access to unlicensed spectrum in LTE release 13," *IEEE Commun. Mag.*, vol. 55, no. 2, pp. 201–207, Feb. 2017.
[3] *Promoting Investment in the 3550—3700 MHz Band*, FCC GN Docket 17-258, Oct. 2018.
[4] *Unlicensed Use of the 6 GHz Band*, document FCC 18-147, Notice of Proposed Rulemaking, Oct. 2018.
[5] *Use of Spectrum Band Above 24 GHz for Mobile Radio Services*, document FCC 16-89, Report and Order and Further Notice of Proposed Rulemaking, Jul. 2016.
[6] *Spectrum Horizon*, document FCC 18-21, Notice of Proposed Rulemaking and Order, Feb. 2019.
[7] I. F. Akyildiz, J. M. Jornet, and C. Han, "Terahertz band: Next frontier for wireless communications," *Phys. Commun.*, vol. 12, pp. 16–32, Sep. 2014.
[8] M. A. Ergin, K. Ramachandran, and M. Gruteser, "Understanding the effect of access point density on wireless LAN performance," in *Proc. ACM MobiCom*, Sep. 2007, pp. 350–353.
[9] *CBRS Coexistence Technical Specifications*, document CBRSA-TS-2001 V2.0.0, Jan. 2019.
[10] J. Jeon and T. Cruz, "Cellular unlicensed spectrum technology," in *Encyclopedia of Wireless Networks*. Springer, 2018, pp. 1–3.
[11] *MulteFire Alliance*. [Online]. Available: http://www.multefire.org/
[12] *NR-Based Access to Unlicensed Spectrum*, document RP-190706, 3GPP TSG RAN Meeting #83, Mar. 2019.
[13] *Statistical Abstract of the United States*, U.S. Census Bureau, Suitland-Silver Hill, MD, USA, 2007.
[14] F. Xu, Y. Li, H. Wang, P. Zhang, and D. Jin, "Understanding mobile traffic patterns of large scale cellular towers in urban environment," *IEEE/ACM Trans. Netw.*, vol. 25, no. 2, pp. 1147–1161, Apr. 2017.
[15] U. Paul, A. P. Subramanian, M. M. Buddhikot, and S. R. Das, "Understanding traffic dynamics in cellular data networks," in *Proc. IEEE INFOCOM*, Apr. 2011, pp. 882–890.
[16] J. Jeon, "NR wide bandwidth operations," *IEEE Commun. Mag.*, vol. 56, no. 3, pp. 42–46, Mar. 2018.
[17] *5 GHz RLAN; Harmonised Standard Covering the Essential Requirements of Article 3.2 of Directive 2014/53/EU*, document ETSI EN 301 893, V2.1.1, May 2017.
[18] *Further Advancements for E-UTRA Physical Layer Aspects (Release 9)*, document 3GPP TR 36.814, V9.2.1, Mar. 2017.
[19] R. Jain, W. Hawe, and D. Chiu, "A quantitative measure of fairness and discrimination for resource allocation in shared computer systems," Sep. 1984, *arXiv:cs/9809099*. [Online]. Available: https://arxiv.org/abs/cs/9809099

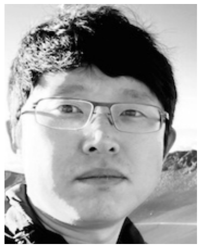

JEONGHO JEON received the Ph.D. degree in electrical engineering from the University of Maryland, College Park, MD, USA, in 2013.

He was with Intel Corporation, Santa Clara, CA, USA, from 2013 to 2018, and worked on various advanced research topics as well as 3GPP 4G LTE and 5G NR standardization. He is currently a Senior Staff Research Engineer with the Standards and Mobility Innovation Laboratory, Samsung Research America, Mountain View, CA, USA, where he explores various 6G candidate technologies. He is the author of more than 30 articles and more than 100 inventions, including pending applications. He was a recipient of the 14th Samsung Humantech Thesis Prize, in 2008, and the National Institute of Standards and Technology (NIST) Fellowship, from 2011 to 2013.

RUSSELL D. FORD (S'09–M'19) received the B.S. degree in electrical and computer engineering from Florida State University, in 2010, the M.S. degree in electrical engineering from the Polytechnic Institute of New York University (NYU), in 2012, and the Ph.D. degree in computer science from NYU, in 2017, under the supervision of Prof. S. Rangan. He is currently a Research Engineer with Samsung Research America, Mountain View, CA, USA. His research interests include next-generation shared spectrum systems, applications of AI for wireless networks, and mobile edge/cloud and ultra-low latency cellular networks.

VISHNU V. RATNAM (S'10–M'19) received the B.Tech. degree (Hons.) in electronics and electrical communication engineering from IIT Kharagpur, Kharagpur, India, in 2012, where he graduated as the Salutatorian for the class of 2012, and the Ph.D. degree in electrical engineering from the University of Southern California, Los Angeles, CA, USA, in 2018.

He is currently a Senior Research Engineer with the Standards and Mobility Innovation Laboratory, Samsung Research America. His research interests include reduced complexity transceivers for large antenna systems (massive MIMO/mm-wave) and ultrawideband systems, in future cellular technologies and in applied artificial intelligence. He is also a member of the Phi-Kappa-Phi Honor Society. He was a recipient of the Bigyan Sinha Memorial Award, in 2012, and the Best Student Paper Award at the IEEE International Conference on Ubiquitous Wireless Broadband (ICUWB), in 2016.

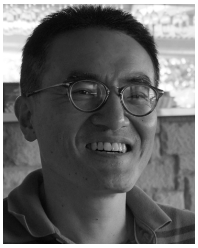

JOONYOUNG CHO received the B.S., M.S., and Ph.D. degrees in electrical engineering from the Pohang University of Science and Technology (POSTECH), South Korea, in 1993, 1995, and 2003, respectively. He was engaged in development of CDMA baseband modem algorithms and FPGA/ASIC chips, while he was with SK Telecom, South Korea, from 1995 to 1998, and as a Research Staff at POSTECH, until 1999. From 2003 to 2018, he was involved with research and standardization for 3G(HSPA)/4G(LTE)/5G(NR) cellular communications, while he was with Samsung Electronics, South Korea, from 2003 to 2015, and Intel Corporation, USA, from 2015 to 2018. He is currently the Senior Director of the Standards and Mobility Innovation Laboratory, Samsung Research America, and leads research and development for 5G and beyond wireless communication systems.

JIANZHONG (CHARLIE) ZHANG (S'00–M'03–SM'09–F'16) received the Ph.D. degree from the University of Wisconsin–Madison, Madison, WI, USA. He was with the Nokia Research Center, from 2001 to 2006, where he was involved in the IEEE 802.16e (WiMAX) standard and EDGE/CDMA receivers. From 2006 to 2007, he was with Motorola, where he was involved in 3GPP HSPA standards. From 2009 to 2013, he has served as the Vice Chairman of the 3GPP RAN1 Group and led the development of LTE and LTE-advanced technologies, such as 3D channel modeling, UL-MIMO and CoMP, and carrier aggregation for TD-LTE. He is currently the Vice President and the Head of the Standards and Mobility Innovation Laboratory, Samsung Research America, where he leads research, prototyping, and standards for 5G cellular systems and future multimedia networks.